# AN IMMUNOHISTOCHEMICAL AND HISTOLOGICAL EVALUATION OF THE AFRICAN BUFFALO (*Syncerus caffer*) RETINA

## A DISSERTATION

### *Submitted as partial fulfilment of the requirements for the degree MMedVet(Ophth)*

**FACULTY OF VETERINARY SCIENCE**

**UNIVERSITY OF PRETORIA**

**ONDERSTEPOORT**

By

Lo-An Odayar
BACHELOR of VETERINARY SCIENCE (UP, Onderstepoort), 2003

**Promoter: Dr I Venter**

**Co-Promoter: Prof L Prozesky**

**Date Submitted: April 2013**

1

# ACKNOWLEDGEMENTS

# DEDICATION

This dissertation is dedicated to my parents, Allan and Valda,

an invaluable source of support and encouragement.

For Koda,

# DECLARATION

4

I, **Lo-An Odayar,** do hereby declare

that the experiment presented in this dissertation

is an original manuscript,

that neither the work nor part of it

has been, is being or shall be submitted for another degree

at this or any other university or institution for tertiary education.

2013

4

# LIST OF CONTENTS

**CHAPTER 1**

**CHAPTER 2**

**CHAPTER 3**

**CHAPTER 4**

**CHAPTER 5**

**CHAPTER 6**

# LIST OF FIGURES

9

## LIST OF TABLES

# GLOSSARY

| WORD | MEANING |
|---|---|
| **Amacrine cells** | These are interneurons in the retina and are responsible for 70% of input to the retinal ganglion cells |
| *Area centralis* | This is the region of the retina in which ganglion cells of a particular functional class concentrate |
| **Bipolar cells** | These cells exist and transmit signals between photoreceptors (rods and cones) and ganglion cells |
| **Bleaching** | Oversaturation of the retinal pigment cells |
| **Chromophore** | A chemical group capable of selective light absorption |
| **Dichromatic colour vision** | This is a two receptor colour perception system |
| **Electroretinography** | Measures the electrical responses of various cell types in the retina, including the photoreceptors |
| **Flicker photometry** | A light intensity study where a single field of view is alternately illuminated by the light sources to be compared |
| **Fovea** | A small depression in the retina of a human eye where visual acuity is highest |

| | |
|---|---|
| **Ganglion cells** | These are neurons located near the inner surface of the retina which receive visual information from photoreceptors via bipolar and amacrine cells |
| **Horizontal cells** | These are lateral interconnecting neurons in the outer plexiform layer of the mammalian retina. They integrate and regulate the input from multiple photoreceptor cells |
| **Immunohistochemistry** | An assay that shows specific antigens in tissues by the use of markers that are either fluorescent dyes or enzymes |
| **Interplexiform cells** | These cells have processes that branch within both the inner and outer plexiform layers |
| ***Kurtosis*** | This is the measure of the "sharpness" of the peak in a frequency distribution curve |
| **Lateral canthotomy** | An operation for lengthening the palpebral fissure by incision through the lateral canthus |
| **Median** | This is the value that is found in the exact middle of a list of values/numbers arranged in numerical order |
| **Mean** | This is the average or central tendency (all the values summed together and then divided by the number of values) |
| **Mode** | This is the most frequently occurring item/value in a list of numbers |

| | |
|---|---|
| **Müller cells** | These are glial cells found in the retina which serve as support cells for the retinal neurons |
| **Opsin** | A protein that forms part of the visual pigment rhodopsin and is released by light stimulation |
| **Photopic vision** | Normal vision in daylight. Vision with sufficient illumination that the cones are active and hue is perceived |
| **Phototransduction** | The process by which light is converted into electrical signals in the rods, cones and photosensitive ganglions |
| **Rhodopsin** | The pigment sensitive to red light in the retinal rods and consists of opsin and retinene. It is also called visual purple |
| **Sample variance** | This is a measure of the distribution of values from the population mean |
| **Scotopic vision** | Night vision or the ability to see in reduced illumination |
| **Skewness** | This parameter describes the asymmetry from the normal distribution in a set of statistical values |
| **Standard deviation** | This value shows the relation that a set of numbers has to the mean of the sample |
| **Standard error** | This is the measure of the accuracy with which a sample represents a population |

# SUMMARY

Vision studies and visual acuity investigations are an ongoing and progressive field in veterinary ophthalmology. These independent studies all help to contribute to a combined and collective knowledge in our understanding of this truly complex matter.

Understanding retinal morphology and physiology is an integral factor in piecing together overall function of the eye. Many of these studies have been done in both medical and veterinary ophthalmology using behavioural factors, electrophysiology, special staining and scanning techniques on a histological level. In the veterinary field many species have been studied pointing out similarities or differences among them. This study hopes to contribute to the understanding of the retinal ultrastructure of the African buffalo (*Syncerus caffer*).

Twenty-five pairs of African buffalo eyes were obtained, but only forty-eight eyes were included in this investigation. The globes of one donor appeared to have chronic intraocular disease and were phthisical. Since this is a descriptive study of normal anatomy and function, these eyes were excluded. Globe dimensions were recorded and statistically analysed, revealing an average horizontal diameter of 32.91mm and a vertical diameter of 33.04mm. The median age of the donor group was 4 years with relatively equal representation of both male and female.

14

Using scanning electron microscopy it was established that African buffalo retinas, like other domestic species, have a specialised region a few millimetres dorsolateral to the optic disc, synonymous to the well described *area centralis*. In this region a higher concentration of cones is found as opposed to other rod-rich regions.

In a concurrent investigation, the contralateral globes were processed for immunohistochemical antibody staining. Colour specific anti-bodies were used to identify the cone population present in the African buffalo retina. The conclusion of this investigation reveals that this species like other domestic animals has dichromatic colour vision, recognising short and medium to long colour wavelengths.

**Keywords:** African buffalo (*Syncerus caffer), area centralis,* rods, cones, dichromatic vision, short wavelength, medium-long wavelength

# CHAPTER 1

## INTRODUCTION

Understanding the organisation of the vertebrate retina has been a common collective goal of visual scientists over the past 30 years. The visual acuity of most domestic animals has been mapped.[1-8] These models together with behavioural studies have led us to widely accepted speculations, concerning certain aspects of vision in some wildlife species.

Considerable progress has been made in the understanding of the ultra-structure and function of the mammalian retina.[9-10] Various morphological techniques including Golgi staining, immunohistochemistry and intracellular staining have led to a greater appreciation of the architecture of this neural structure.[9] Functional studies on the other hand, have been further elucidated using electrophysiology, particularly electroretinography.[11]

### 1.1 Colour Vision in the Bovine

Earlier reviews have noted the inclusion of bovines and other ungulates in colour vision experiments.[2] These studies had the common outcome that all of the ungulates tested showed some ability to make colour discriminations. What they also had in common was that in no case was there the sort of documentation that would lead to a categorisation either of the nature of the colour vision in an ungulate or of its mechanism.

Electroretinogram flicker photometry was used in a study to measure the spectral properties in three common ungulates – cattle (*Bos taurus*), goats (*Capra hircus*) and sheep (*Ovis aries*). The location of two cone mechanisms was identified and qualified. The S-cone mechanism varied from about 444-455nm for the three species. The M/L cone mechanisms were tightly clumped at about 552-555nm. From this it was deduced that these species have the requisite photopigment basis for dichromatic colour vision.[6]

Visual stimuli have been shown to be more important to the bovine when acquiring feed, than are auditory inputs.[28] Numerous behavioural studies related to bovine colour vision have been carried out, some with conflicting results relating to the ability to differentiate colours from each other or between shades of grey.[4, 5, 29] In one study involving 8 adult cows of the Spanish fighting breed, behavioural testing supported the theory that cattle can easily differentiate the longer wavelengths (550-700nm) from grey, but have greater difficulty with the shorter wavelengths (400-500nm). In the same study it was also concluded that anatomical differences in the density of cones and differences in biochemical composition of the photoreceptors, might lead to variations in colour perception among various bovine breeds.[4]

To date, it appears that no documented scientific research is available which describes the retinal photoreceptor ultrastructure of our wildlife species, in particular the African buffalo. Bovine eyes in general have provided the raw materials for innumerable experiments on the biochemistry and biophysics of

17

rod photoreceptors.[30-32] However, despite this, very little is known of the cones and cone-based vision in these animals and related species.

1.2 Problem Statements

1. Retinal architecture in the African buffalo has not been studied with specific reference to rod and cone concentrations and ratios in specific topographical regions within the retina.

2. No documented evidence regarding the colour visual spectrum at the ultrastructural level for the African Buffalo is currently available.

# CHAPTER 2

## OBJECTIVES

2.1 Objectives of the study

1. To determine the concentration of rods and cones at two predetermined locations (10mm dorsolateral to the optic nerve and 10mm dorsomedial to the optic nerve) in the retina of the African buffalo.

2. To determine the rod to cone ratios in the two above-mentioned locations.

3. To identify the spectral sensitivity of the African buffalo cone pigments by using cell-specific antibodies.

2.2 Benefits arising from this study

1. The results of this project will contribute to a better understanding of the visual spectrum of the African buffalo.

2. The findings of this project will provide a platform for further research into the retinal architecture of the African buffalo and other wildlife species.

3. This project will form part of the research requirements of Dr LT Odayar's MMedVet (Ophth) degree.

2.3 Hypothesis

1. **The distribution of rods and cones is not uniform throughout the retina, consistent with other mammalian species, with a higher rod density in the region dorsomedial to the optic nerve.**

2. **The African buffalo has a region similar to the *area centralis* found in most mammalian retinas where the cone concentration is higher compared to the rest of the retina.**

3. **The African buffalo has dichromatic vision with cone wavelength spectral sensitivities of 450nm and 550nm, respectively for the short and medium to long –wavelength sensitive cones respectively.**

# CHAPTER 3

## LITERATURE REVIEW

### 3.1 Functional Anatomy of the Neural Retina

The neural retina consists of six types of neurons:

1.   Photoreceptor cells (rods and cones)

2.   Horizontal cells

3.   Bipolar cells

4.   Amacrine cells

5.   Müller cells

6.   Ganglion cells
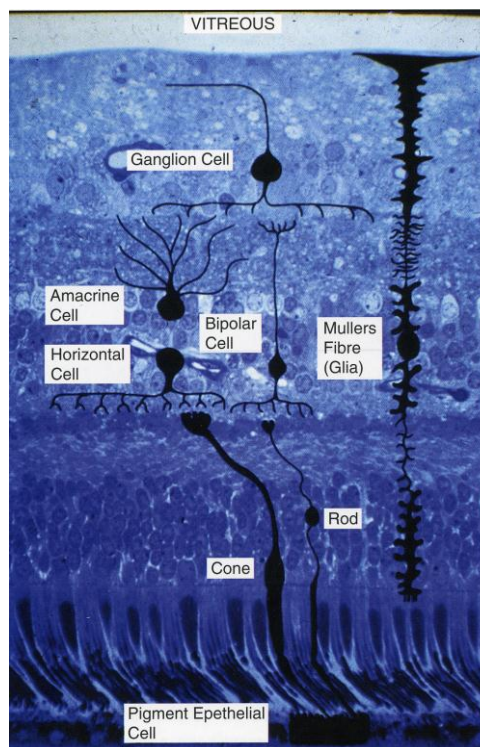


**Figure 3.1.** Distribution of the six types of neurons in the vertebrate retina.

Courtesy of PR Wheater.

Using light microscopy, ten parallel cell layers can be distinguished from the outward side of the retina, inwards:

1.    Retinal pigment epithelium (RPE)

2.    Outer and inner segments of rods and cones

3.    Outer limiting membrane (OLM), which is not a membrane, but a row of zonulae adherents connecting photoreceptor cells to Müller cells and Müller cells to one another

4.    Outer nuclear layer (ONL), which consists of fibres and cell bodies of photoreceptor cells

5.    Outer plexiform layer (OPL), where photoreceptors, horizontal and bipolar cells synapse with one another

6.    Inner nuclear layer (INL), which is occupied by the cell bodies of horizontal, bipolar, amacrine and interplexiform cells

7.    Inner plexiform layer (IPL), where bipolar, amacrine and ganglion cells synapse with each other

8.    Ganglion cell layer (GCL), which is occupied by the cell bodies of ganglion cells and displaced amacrine cells

9.    Layer of optic nerve fibres (OFL), which is occupied by the ganglion cell axons as they course over the inner surface of the retina to reach the optic nerve disc

10.   Inner limiting membrane (ILM), which is a basal lamina connecting the foot processes of Müller cells to the vitreous body
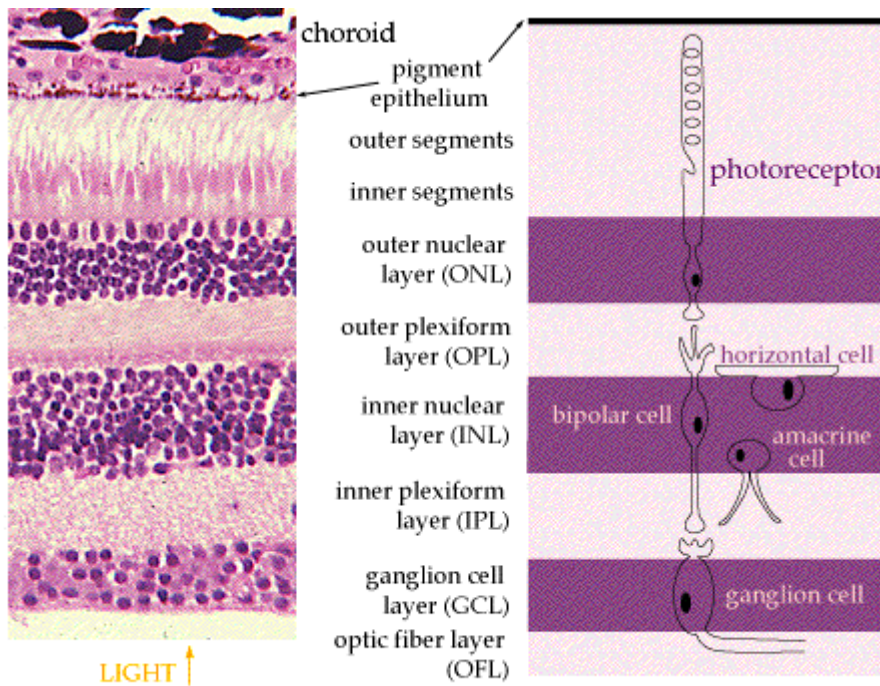
**Figure 3.2.** The ten parallel cell layers of the retina. Courtesy of PS Bernstein.

3.2 Photoreceptors

Rod and cone photoreceptors are best regarded as neurons with outer and inner segments that are highly specialised. These segments, which are cylindrically to conically shaped, are closely packed together, side by side, and are arranged radially and parallel to incoming light. The segments react to the stimulation of light and initiate the mechanism of vision as well as the reflexes associated with it.

23
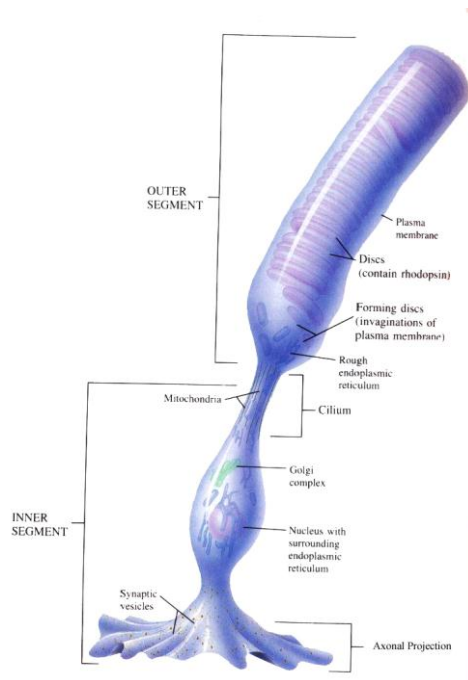
**Figure 3.3.** Schematic representation of the inner and outer segment of the rod photoreceptor. Courtesy of T. Caceci 1998.

The axon terminals of the photoreceptors exhibit expansions; the rod expansions are roughly spherical in shape and are termed rod spherules, whereas the cone expansions spread more widely and are termed cone pedicles. The outer segments of rods and cones are composed of stacks of membranous discs surrounded by a cell membrane. The rods form stacks of uniform width throughout their length and are thus longer than the cone outer segments. The cone outer segments appear to be wider at their inner end, producing a cone shape.[1]

24

ROD                                            CONE
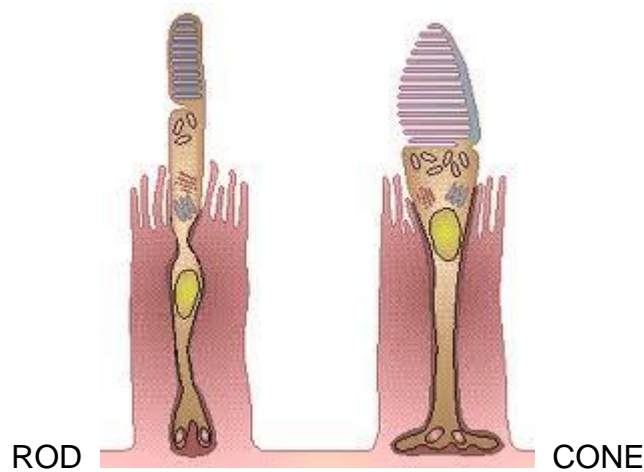
**Figure 3.4.** Diagrammatic illustration of the morphological differences between rods and cones. Courtesy of Benjamin Cummings (2007).

The membranous discs which constitute the rods and cones are in fact flattened spheres. They consist of two membranes that are continuous at their ends and, in rods, are separate from the cell membrane as well as the adjacent discs. In some mammalian cones, the proximal discs have continuity with the cell membrane, but it is uncertain how accurate this generality is among mammals.[2] However, this invagination of the cell membrane, which is also known as the disc lamella, constitutes the major morphologic difference between rods and cones.

25
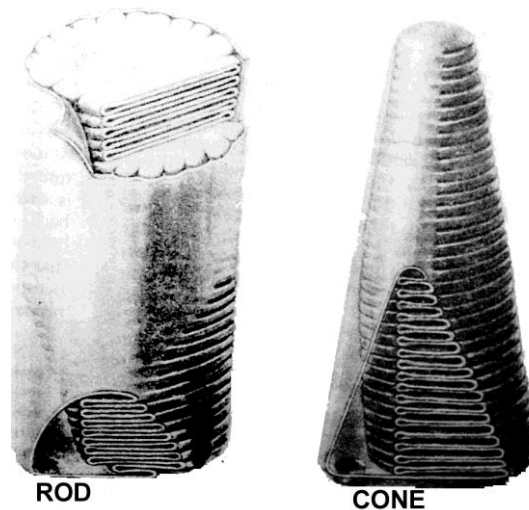
**Figure 3.5.** Morphological differences between rod and cone cell membranes (outer segment). Courtesy of Young (1971).

The layer of the visual cell nuclei varies somewhat in thickness depending on the retinal location from 9-13 rows centrally to 7-9 rows peripherally in the feline.[3] The cone nuclei, with dispersed chromatin, are somewhat larger and more circular than the rod nuclei, with more homogenously arranged chromatin and are located in the outer row of the ONL.

The slender rod outer segments are more sensitive to light than cones. Rods function more effectively in low illumination (scotopic vision) and are inactivated by bright light and are thus well suited for night vision. On the other hand, they have less resolving power and produce a considerably lower visual acuity.[1]

Cones are useful for vision during daylight (photopic vision) and can rapidly adapt to repeated stimuli. They are however less sensitive to light and

26

therefore do not respond to low light levels. Within each mammalian cone outer segment, the discs contain one of three photopigments, which are sensitive to one of three different wavelength ranges.[1] Birds, by comparison, possess four or even five classes of cone photopigments.[4] Spectral sensitivity studies on human cone pigments have shown cone pigments which absorb photons in 3 regions of light spectrum: 419nm (blue), 531nm (green) and 558nm (red).  Blue cones represent about 10% of the total cone population and are absent in the central most region of the fovea, whereas green cones represent about 54% and red cones about 33%. Most other mammals possess at least 2 classes of photopigments: those sensitive to one short wavelength and those sensitive to one or more long wavelength.[5] In the feline retina cone peak sensitivity has been found to be at 450 and 550nm for blue- and green-sensitive cones respectively using electrophysiological studies. There are also suggestions that the feline may be trichromatic, with an additional class of cones peaking at 520nm.[6] Immunocytochemical studies in mice retinas have shown an even distribution of two cone types, which separates the retina into two fields by an oblique meridional line.[7] The middlewave sensitive cones (M-cones) were present exclusively in the dorsal half of the mouse retina, while the majority of the shortwave-sensitive cones (S-cones) occupied the ventral half of the retina.
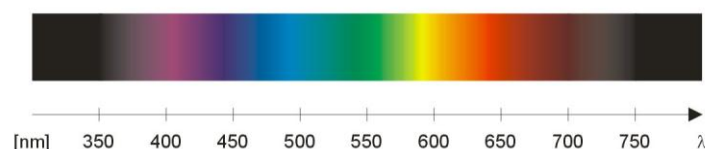


**Figure 3.6** Colour spectral ranges with the corresponding wavelength values

The distribution of rods and cones is not uniform throughout the retina in different species, and this topographic specialisation is particularly pronounced in primates.[8] The primate retina possesses a depression or fovea where visual resolution is maximal. There are only cone photoreceptors in this area and they attain their highest density because of their small diameter, specifically in this location, also the deep retinal layers are displaced towards the margins of the depression, where the postreceptor neurons have an especially high density. In the feline there is also a specialised region, dorsotemporal to the disc, the *area centralis*, which is not rodless but where the rod to cone ratio is lower and the density of photoreceptors and postreceptor neurons is higher than in other retinal areas. The rod-cone ratio in the *area centralis* is 10:1 whereas it is 65:1 in the peripheral feline retina. A visual streak can be depicted in the feline retina that extends horizontally on either side of the *area centralis*. Rod outer segment diameter ranges form 1-1.6 microns in the cat. In the area centralis the rod outer length is 15 microns in the adult feline. In the rabbit there is also an elongated horizontal region, or visual streak, situated below the optic nerve head and medullary rays in which area the density of retinal cells is highest. In this region, however, the cone to rod ratio is the same as in the rest of the retina. Rodents possess rod-dominated retinas, in which about 3% of the photoreceptors have been found to be cones, without any marked difference in distribution.[9]

Cone photoreceptors account for colour vision and many vertebrate species are able to enjoy a world of colour since their visual systems include more than one type of wavelength selective photoreceptor. Teleost fish, birds and

reptiles are extremely colour sensitive and have tetravalent visual systems with sensitivity spanning a large part of the spectrum from the far red to the ultraviolet ends. Amphibians and mammals have divariant colour vision systems. Most primates, including man, have trivariant colour vision. The perception of colour, however, varies complexly as a function of multiple parameters, including the spectral composition of light coming from the object, the spectral composition emanating from the surrounding objects and the state of light adaptation in the subject just prior to viewing any given object.

## 3.3 Physiology of the photoreceptors

### 3.3.1 Phototransduction

- Retinal pigments

The process of vision begins with the absorption of a photon by a photopigment in the outer segment of the photoreceptor. A visual photopigment consists of two parts. The first is opsin, which is an apoprotein that determines the wavelength of the photon the pigment will absorb. The second is a vitamin A1 - derived chromophore molecule, 11 -*cis* - retinaldehyde (retinal).

The photopigment of rods, known as rhodopsin, is an integral part of the membrane of the outer segment discs. Rhodopsin is a long polypeptide chain that traverses the disc membrane as a helix. It has been estimated that each

29

rod has approximately $10^9$ rhodopsin molecules.[10] In most mammalian species studied to date, absorption by rhodopsin occurs between 495nm and 500nm.[11]

Cone pigments such as iodopsin, do not appear to be similar to rhodopsin in either structure or function.[12] In humans there are three different iodopsins that form the protein-pigment complexes photopsin I, II, and III. They are called erythrolabe, chlorolabe, and cyanolabe, respectively. These photopsins have absorption maxima for yellowish-green (photopsin I [500-700nm]), green (photopsin II [450-630nm]), and bluish-violet light (photopsin III [400-500nm] ).

In rods and cones as a photon is absorbed by the pigment, 60% of its energy is transferred to the pigment molecule. This energy is then used to initiate a chain bleaching reaction, which results in the breaking away of the opsin segment and subsequently the photoisomerisation of the chromaphore into all - *trans* - retinaldehyde, or R*. This bleaching process is also known as the early receptor potential.

- Depolarisation and hyperpolarisation

Photoreceptors are unique cells in that they are depolarised in their resting state (darkness). This depolarisation is maintained by a dark current, which is essentially a constant influx of $Na^+$ through cyclic guanosine-3, 5- monophosphate (cGMP) - gated ion channels in the outer segment membrane.

The end result of light stimulation is an overall decrease in cGMP levels, leading to closure of the ion channels. The closure of these channels results in cessation of $Na^+$ influx, allowing the cell to undergo hyperpolarisation

The cGMP cascade of phototransduction is characterised by the isomerisation of the photopigment by light into R*. This bleached molecule then binds to transducin, which is a G protein composed of subunits ($T\alpha$, $T\beta$ and $T\gamma$), bound to guanosine diphosphate (T-GDP) under states of darkness.

This new complex, T-GDP-R*, eventually loses its affinity for GDP due to the binding process and leads to the replacement of GDP by GTP (guanine triphosphate), leading to the formation of a T-GTP-R* complex.

The formation of this complex leads to further affinity changes and subsequently the complex dissociates. R* falls off and becomes free again to activate additional T-GDP molecules. $T\beta$-$T\gamma$ also dissociates from the complex. $T\gamma$ is known as the inhibitory subunit, therefore loss of this sub-complex activates the $T\alpha$-GTP molecule which remains.

The activated complex then migrates to the disc membrane where it is involved with the activation of phosphodiesterase ( PDE ), by removing its $\gamma$ inhibitory subunits. Because PDE contains two $\gamma$ subunits, two $T\alpha$-GTP complexes are required for complete PDE activation.

The activation of PDE allows for the hydrolysis of cGMP into GMP. This leads to a subsequent decrease in cGMP levels ( from $60\mu M$ to $< 10\mu M$) which then leads to the closure of the Na+ channels and subsequent hyperpolarisation.

Each R* molecule can activate up to 500 T-GDP complexes and each activated PDE molecule may hydrolyse 800 cGMP molecules. Taking into account that two T$\alpha$-GTP complexes are required for complete PDE activation, the net result of amplification of a single signal is by a factor of 100,000.

A complex chain reaction exists to "turn-off" the cGMP cascade of phototransduction. T$\alpha$-GTP is hydrolysed into T$\alpha$-GDP and in turn the PDE inhibitory $\gamma$ subunit is made available again to rebind the PDE. This process inhibits the hydrolysis of cGMP.

The T$\alpha$-GDP molecule also rebinds the T$\beta$-T$\gamma$ subunits and the transducin molecule becomes deactivated. R* undergoes phosphorisation, which enables it to bind to arrestin. This proccess prevents further transducin activation by R*. Guanylate cyclase activity also increases in the outer segment and this leads to synthesis of cGMP and eventually causes reopening of the Na+ - gated channel.
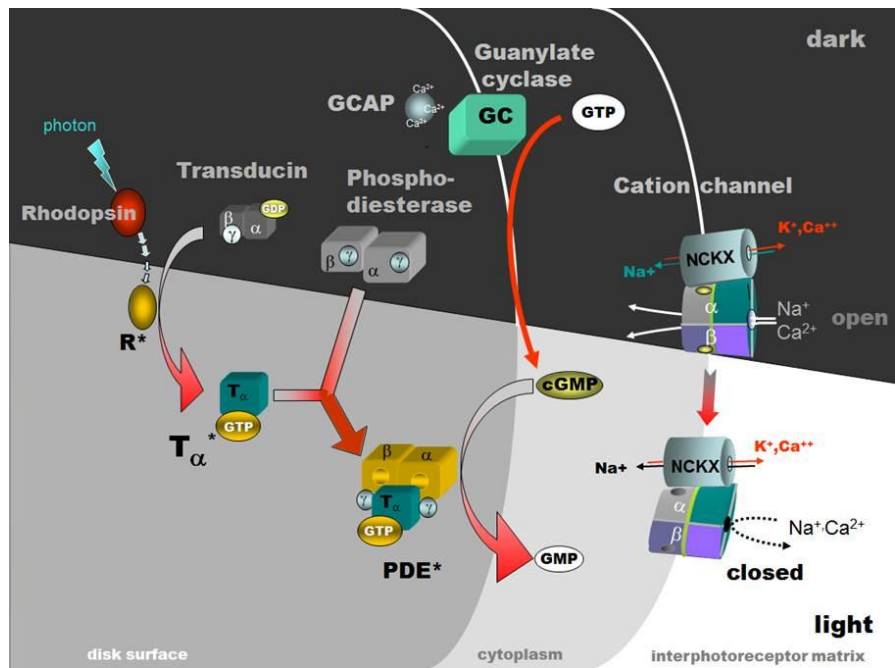
**Figure 3.7.** Activation of rhodopsin by light and the phototransduction cascade. Courtesy of Wolfgang Baehr.

- Synthesis and regeneration of the visual pigments

Light stimulation results in bleaching of the photopigment. These bleached pigments undergo a process of regeneration during states of darkness. There is a constant dynamic process of bleaching and regeneration which occurs, allowing an equilibrium to be set with adaption to existing light levels.

The first step in photopigment regeneration involves the reduction of all-*trans*-retinal to all-*trans*-retinol. This step occurs in the outer segment of the photoreceptor. The rest of the cycle takes place in the retinal pigment epithelial layer (RPE).[13]

33

Retinol diffuses from the outer segment into the subretinal space and makes its way through the RPE. Intercellular movement of retinol is made possible by an interstitial retinoid-binding protein (IRBP).[14] The exact process of this mechanism is yet to be completely understood.

Retinol becomes esterified in the RPE into retinyl and this molecule eventually becomes isomerised into 11-*cis*-retinaldehyde. This molecule is translocated again by IRBP from RPE back into the outer segment where it is able to bind with opsin, which is synthesised in the inner segment, to reform rhodopsin.[15,16]

This bound protein is then transported through the bloodstream and eventually reaches the *choriocapillaris*. The retinol is then taken up by certain receptors on the outer RPE and processed in a similar way as descibed above.
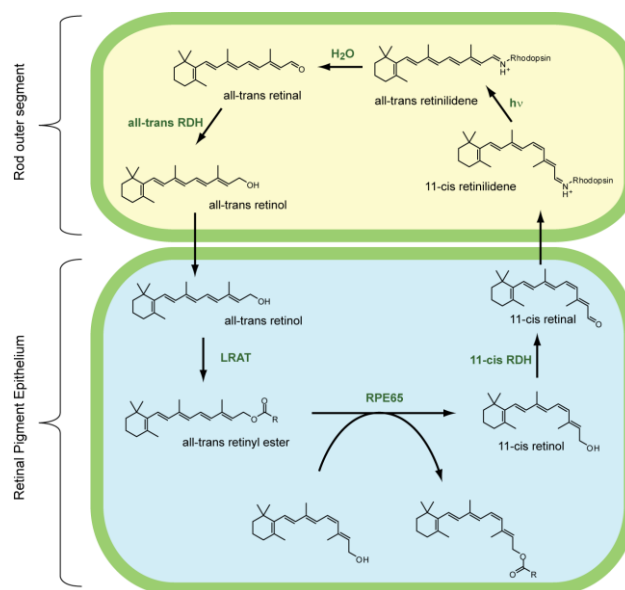


**Figure 3.8.** Regeneration of the visual pigment. Courtesy of L Joespeh (2003)

34

## 3.4    <u>Immunohistochemistry</u>

Immunohistochemistry or IHC refers to the localization of antigens in tissue sections. Labeled antibody reagents are used to create specific antigen-antibody interactions in the tissue being studied.

Visualising an antibody-antigen interaction can be accomplished in a number of ways. In the most common instance, an antibody is conjugated to an enzyme, such as peroxidase, that can catalyse a colour-producing reaction. Alternatively, the antibody can also be tagged to a fluorophore, such as fluorescein or rhodamine

 IHC is widely used in basic research to understand the distribution and localization of biomarkers and differentially expressed proteins in different parts of a biological tissue. Immunohistochemistry involves specific antigen-antibody reaction and has the apparent advantage over traditionally used special enzyme staining techniques that identify only a limited number of proteins, enzymes and tissue structures.

### 3.4.1  History of immunohistochemistry

Albert H. Coons and his colleagues (Coons et al. 1941, 1955; Coons and Kaplan 1950) were the first to label antibodies with a fluorescent dye, and use it to identify antigens in tissue sections. With the expansion and development of immunohistochemistry technique, enzyme labels have been introduced such as peroxidase (Nakane and Pierce 1966; Avrameas and Uriel 1966) and alkaline phosphatase (Mason and Sammons 1978). Colloidal gold (Faulk and Taylor 1971) label has also been discovered and used to identify immunohistochemical reactions at both light and electron microscopy level. Other labels include radioactive elements, and the immunoreaction can be visualized by autoradiography.

### 3.4.2  Retinal Immunohistochemistry

Retinal cones have wave-length-specific visual pigments. To identify subclasses of cones, opsin-specific antibodies have been used successfully to date.

 The full range of colour discrimination in humans has been mapped using immunohistochemistry. These principles are based on the presence and function of three cone photoreceptor mechanisms. Each cone type possesses a photo-sensitive pigment-protein complex consisting of 11-cis retinal and a

36

unique opsin protein, which gives sensitivity in the short (S cone, peak sensitivity about 420nm), middle (M cone, peak sensitivity about 530nm with polymorphism; Winderckx et al., 1993; Neitz & Neitz, 1998), and long (L cone, peak sensitivity about 560nm with polymorphism; Neitz & Jacobs, 1990) wavelengths of the light spectrum.

In a similar study in the canine retina, short and medium opsins were expressed by the majority of cones in the retina, both within the area centralis and in the peripheral retina.

Bovine retinas have been used in a number of immunohistochemical research studies. These studies centered on descriptive studies of the retinal pigment epithelium and various growth and hormone receptor expression. No studies to date categorize the cone photoreceptor population of the bovine retina using immunohistochemistry. The same statement is true for the African buffalo cone photoreceptors.

**CHAPTER 4**

MATERIALS AND METHODS

4.1 Model system and justification of the model

This study will include twenty-five (25) pairs of African buffalo eyes. The African buffalo is a species that is flourishing in our National Parks and according to the Parks Board, which oversees the Kruger National Park, groups of these animals are culled from time to time for routine Tuberculosis and Foot and Mouth testing. The rest of these carcasses then become available for the furthering of scientific research and development. The eyes of these animals are currently not being used by any other scientific research venture; this would then be a valuable opportunity to use these specimens constructively to gain some insight on retinal architecture and photoreceptor activity in these animals.

The 25 pairs of eyes were collected in August 2005 following the approval of a provisional protocol submitted in May 2005, (**Appendix 1**). The reason for this was because of the upcoming culling season where many carcasses became available for scientific research purposes. Permission was granted to harvest fresh eye specimens and provisionally preserve and process them for further investigation following the approval of the intended research protocol.

**Figure 4.1.** Field data collection and primary sample processing

4.2 Experimental design

On removal of the eyeballs, the following data was recorded: date, identification number, donor gender, donor age, left and right globe diameter: dorsal to ventral and lateral to medial respectively. These values are recorded in **Appendix 2**.

Electron microscopy will be used to determine the ratio of rods to cones in two predetermined areas of the retina. These areas will be 10mm dorsolateral to the optic nerve and 10mm dorsomedial to the optic nerve.

39

The dorsolateral region is chosen as the presumed cone-rich *area centralis* and the dorsomedial region is harvested as a control sample, representative of the rest of the retina.

Immunohistochemistry will be used to determine the wavelength spectrum to which the cones of the retina are sensitive.

Three regions of wavelength spectrum (red, green and blue) will be tested throughout the retina samples to either prove or disprove the proposed hypothesis of dichromatic vision in the African buffalo

## 4.3 Experimental procedures

### 4.3.1 Harvesting the specimens

Within a few minutes after a group of twenty-five buffalo were culled, the eyes were enucleated using the standard subconjunctival approach without performing a lateral canthotomy, so as to preserve the surrounding skin and eyelids. A description of the procedure follows.

Beginning in a dorsal quadrant, bulbar conjunctiva was incised approximately 5mm posterior to the limbus. The conjunctiva and Tenon's capsule were then bluntly dissected and undermined from the globe. The extraocular muscles were identified and transected close to their scleral insertions. The globe was then mobilised and displaced in a forward direction. The *retractor bulbi* muscle

40

was identified and transected in a similar fashion to the other extraocular muscles. The globe was then rotated medially to expose the optic nerve, which was clamped with a curved haemostat. The nerve was then transacted 5mm behind the posterior end of the globe. The haemostat was then removed.



**Figure 4.2.** African buffalo globe following enucleation

4.3.2 <u>Processing the specimens</u>

Once removed and the various measurements recorded, the right eye was immediately placed into a glutaraldehyde bath. While immersed in glutaraldehyde, the eye was opened, using a pair of sharp scissors, in a 360-degree fashion approximately 5mm caudal to the limbus. This procedure separated the anterior segment of the globe from the posterior. The vitreous was allowed to flow out into a bottle of formalin, appropriately labelled with the animal's identification number. The cornea, lens and iris were placed into the same bottle.

41

The posterior section of the globe was then placed onto a dental wax base immersed in glutaraldehyde. Using a 5mm biopsy punch, two samples were taken from the retina. The samples were taken approximately 10mm medial and lateral to the optic nerve respectively. The retinal samples were then pinned to a 5mmx5mm block of dental wax, marked appropriately and placed into a glutaraldehyde-containing specimen bottle, labeled with the corresponding animal identification number. These samples were then submitted to the Electron Microscopy Unit (Onderstepoort), for storage until further processing. The rest of the posterior section of the globe was placed into the formalin bottle already containing the vitreous and anterior segments.
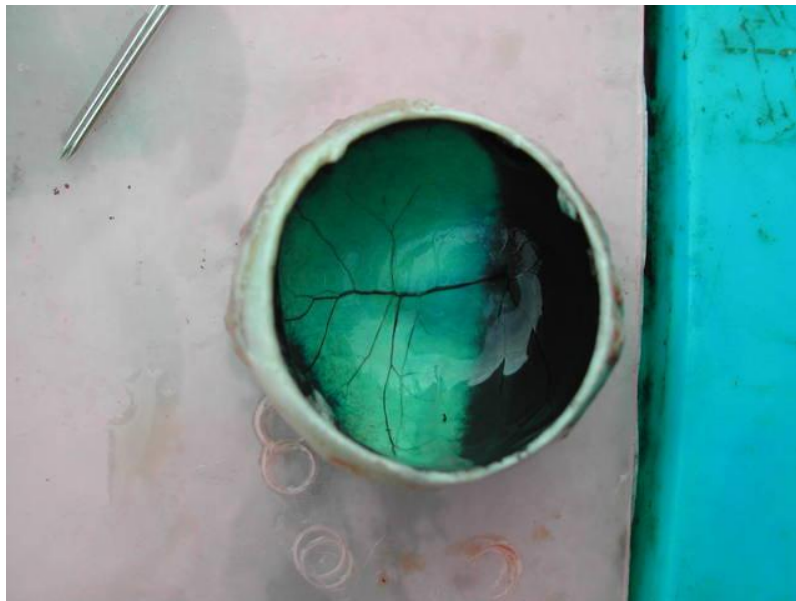


**Figure 4.3.** The posterior section of the right globe on a dental wax base.

**Figure 4.4.** 5mm punch biopsy sampling of the retina of the right globe.



**Figure 4.5.** Retinal punch sample prior to mounting on dental wax block
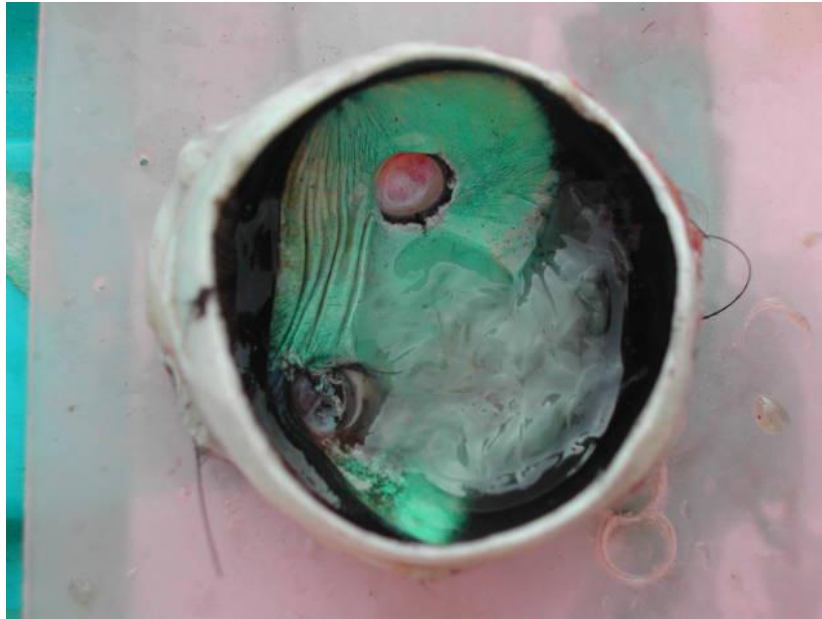
**Figure 4.6** The remaining posterior segment post sampling.

### 4.3.3 Electron Microscopy

The retinal samples in glutaraldehyde were processed in preparation for viewing by the scanning electron microscope. The glutaraldehyde-fixed samples were removed from the specimen bottles and placed into a buffer solution for 10 minutes. These samples were then rinsed thoroughly in distilled water and subjected to a dehydrating process as follows:

- 50% ethanol for 15 minutes, then
- 70% ethanol for 15 minutes, then
- 80% ethanol for 15 minutes, then
- 90% ethanol for 15 minutes, then
- 96% ethanol 15 minutes and finally
- 100% ethanol for 30 minutes.

44

The samples were then placed into sample holders and subjected to critical point drying after which they were mounted onto round aluminum stubs using carbon adhesive tabs. The samples were then splutter coated and viewed using a scanning electron microscope.

For each sample, the numbers of rods and cones were counted and recorded on the appropriate data capture table. The count was carried out along the cut surface of the sample at a 100,000 magnification at 20 kv in a single high powered field.

Figure 4.7 below is a scanning electron microscope slide from donor 187. This section was a sample from the medial retinal sample pool. The figure shows a total rod count along the cut surface of 19 rods and 2 cones.
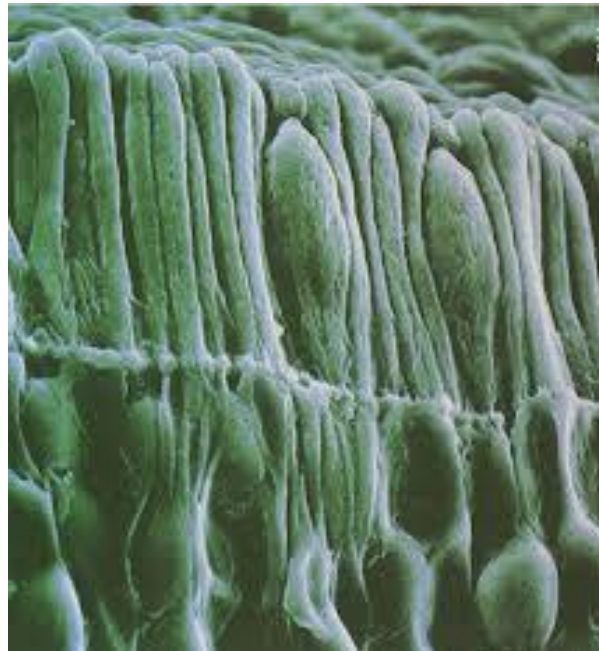


**Figure 4.7** Scanning electron microscopy view of the rods and cones (donor 187 – medial retinal sample)
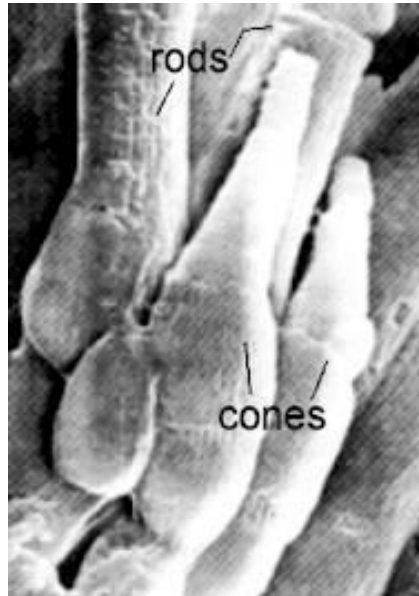
**Figure 4.8** A close-up view of individual rods and cones using electron microscopy (Courtesy of www.eyedesignbook.com/ ch3/eyech3-i.html)

### 4.3.4 Immunohistochemistry

The left eye, removed from the same animal, was trimmed of all excess extra-ocular tissue (muscle and fat) and the globe diameter measurements recorded. The eyeball was then immersed in 10% buffered formalin for fixation. These specimens were then submitted to the Pathology Department (Onderstepoort) for further processing and cutting in preparation for immunohistochemical staining.

Formalin-preserved eyeballs were transected at the *ora ciliaris retinae.* The anterior segment, lens and vitreous body were preserved in formalin together with the corresponding segments of the right eye. These samples will be kept safely for use in further research should it be required. The remaining

46

eyecups were then rinsed and cryoprotected by transferring them stepwise through solutions of increasing concentrations of sucrose (10, 15 and 20%) in Sorensen's buffer. The samples were then embedded in Yazola media (30% egg albumen and 3% gelatine in water) and mounted for sectioning. Sections, 12 microns thick, were cut in a cryostat from the central part towards the periphery, in a vertical plane, comprising a total width of about 2mm horizontally. The individual sections were collected on chrome alumcoated slides and air-dried. These were then stored at -20 degrees Celsius until used.

Three sections from each donor were randomly selected. Each one of these sections were treated with one of three anti-opsin stains (see below) in the following manner:

The sections were then thawed rapidly at room temperature and washed in phosphate-buffered saline at pH 7.2 (PBS). Bovine serum albumin (1%) was then added to the PBS. This was essential for the dilution of the antibodies. The sections were then incubated in the appropriate dilution for 16-18 hours at 4 degrees celsius. Following this the slides were then left at room temperature for one hour and then rinsed in PBS and further incubated for 45 minutes in darkness with the second antibody. This process was repeated for the third antibody.

The slides were then mounted in anti-fading mounting medium. [33] The slides were examined using a fluorescence microscope. The presence or absence

of each of fluorescence for each of the three secondary antibodies was recorded for each section.

- Immunohistochemical antibody stain selection

Three antibodies were chosen for this study.

  - AB5407, rabbit anti-opsin blue polyclonal antibody in PBS {0.02M phosphate, 0.25M NaCl, pH 7.6} with 0.1% sodium azide as a preservative.

One slide from each donor stained with AB5407 showed the following florescence :-
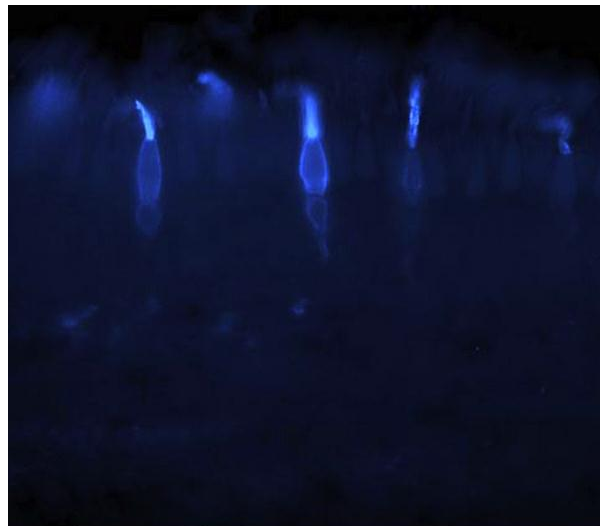


**Figure 4.9** Florescence microscopy slide from donor 207 (Slide 55) showing the presence of short (blue sensitive) cone photoreceptor cells

The presence of this antigen-antibody complex florescence confirms the short cone wavelength photoreceptor inclusion in the African buffalo retina

48

- AB5405, a green anti-opsin antibody (Purified rabbit polyclonal in buffer containing PBS, 0.02 M phosphate, 0.25 M NaCl, pH 7.6 with 0.1% sodium azide.). The presence of this antigen-antibody complex florescence also confirms the inclusion of medium cone sensitive photoreceptor cells.

One slide from each donor was stained with AB5405 and showed the following florescence;-
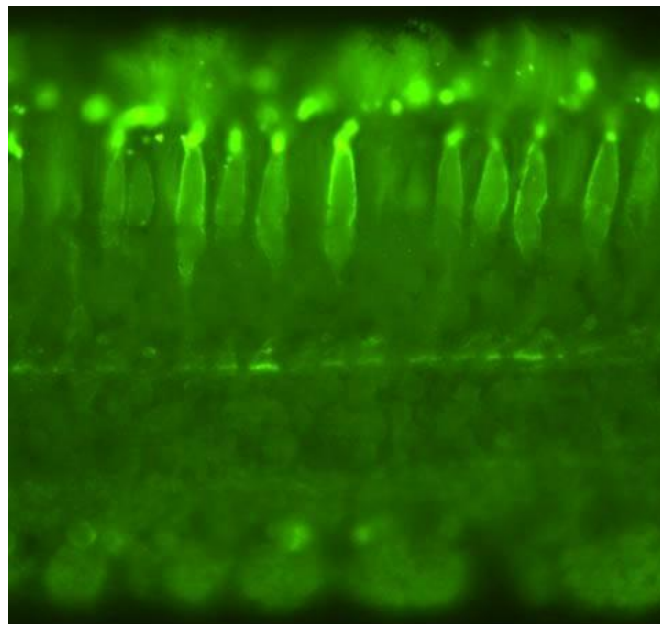


**Figure 4.10** Florescence microscopy image from donor 193 (Slide 24) of medium length cone photoreceptor antibody-antigen complexes.

49

- AB5745, affinity purified immunoglobulin, in PBS containing 0.02% sodium azide.

One slide from each donor was stained with AB5745 and a noticeable absence of florescence with this stain complex was noted. This confirms the absence of long wavelength or red sensitive cone complexes in the test sample.
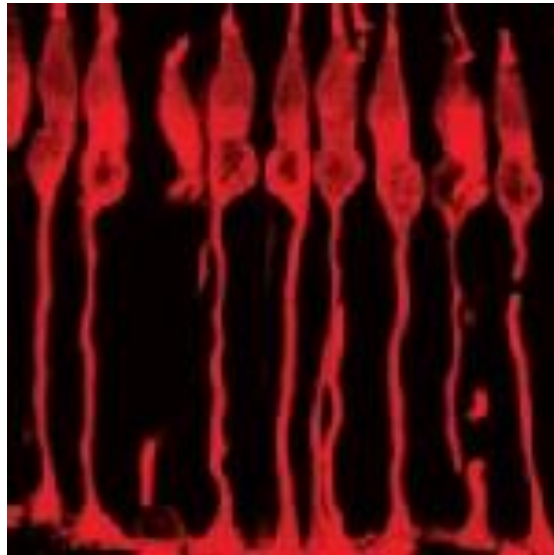


**Figure 4.11** Human red (long-wavelength) cone photoreceptor florescence[35]. This antigen – antibody complex was absent in the African buffalo stain analysis

## 4.4 Data Analysis

A statistical evaluation of all data recorded will be done. All data obtained will be hand recorded using data capture sheets as shown under **Appendix 2, 3 and 4.** This data will then be transferred to Microsoft Excel spreadsheets, using a personal computer. This data will then be statistically analysed using XLSTAT. All data will be stored on back-up compact discs, which will be kept by the investigator.

Descriptive statistics will be used to evaluate all data captured. Mean values as well as mode and median will be calculated. Standard error and deviations together with sample variation, skewness, kurtosis and range will be discussed for specific parameters. Graphical representations will also form part of the description of recorded findings.

# CHAPTER 5

## RESULTS

### 5.1 Sample population

Twenty-five pairs of African buffalo eyes were acquired and prepared for data processing. While recording the initial set of parameters in **Appendix 2**, it was noted that the globes from donor 184 were comparably smaller to those from donors of a similar age and gender. Closer inspection revealed that these globes were phthisical as a result of previous ocular disease. These samples were excluded from the study.

Globe diameter measurements (both dorsal to ventral and lateral to medial) were recorded in millimetres for forty-eight eyes. These samples came from relatively equal groups of both male and female with ages ranging from three to five years. These statistical results are illustrated in **Table 1**.
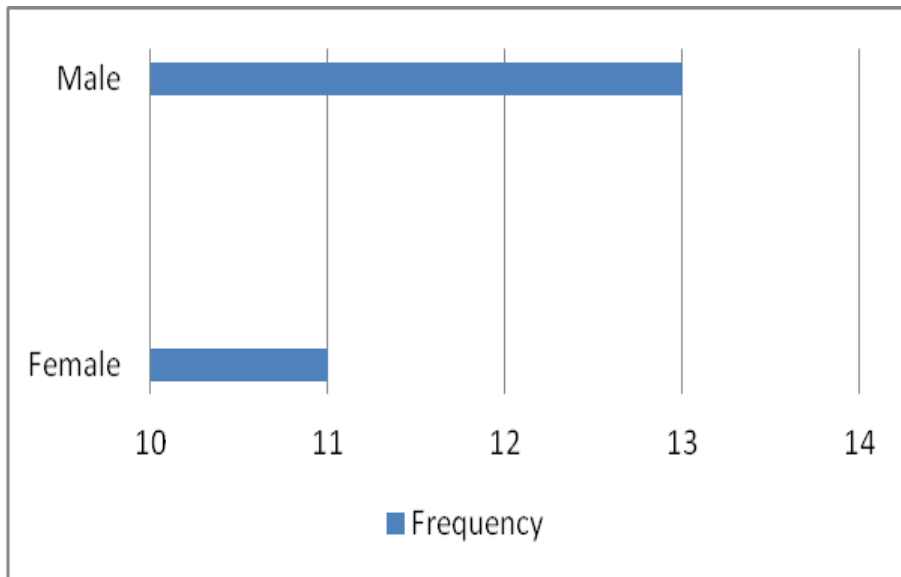
**Figure 5.1.** Histogram representing the gender distribution in the sample population
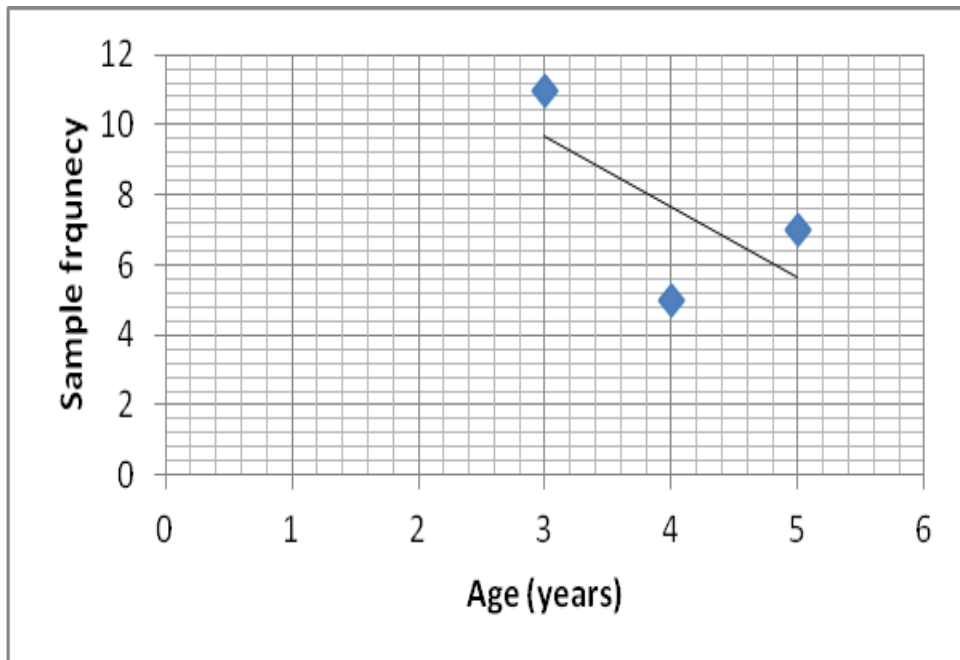


**Figure 5.2.** X-Y scatter plot representing the age groupings in the population group

53

The central tendency for globe diameters, as determined by the mean values calculated, is noted at 33.04mm (dorsal to ventral) and 32.91mm (lateral to medial). Median and mode values for these parameters were relatively similar indicating an even distribution of measurements across this sample population, with only a very slight asymmetry around the central tendency. This is indicated by the skewness value of -0.9 and -0.7 for dorsal to ventral and lateral to medial respectively. A flatter kurtosis value (-0.22) is seen with the lateral to medial measurement distribution over the population, whereas with the dorsal to ventral reading (0.35) tend to peak slightly towards the central tendency.

**Table 1.** Descriptive statistics generated form donor signalment and sample measurements.

| Variables | Age | DV | LM |
|---|---|---|---|
| Mean | 3.826087 | 33.04255 | 32.91489 |
| Standard Error | 0.184928 | 0.381047 | 0.29146 |
| Median | 4 | 34 | 34 |
| Mode | 3 | 35 | 34 |
| Standard Deviation | 0.886883 | 2.612324 | 1.998149 |
| Sample Variance | 0.786561 | 6.824237 | 3.992599 |
| Kurtosis | -1.67841 | 0.349231 | -0.22801 |
| Skewness | 0.367484 | -0.91202 | -0.69751 |
| Range | 2 | 4 | 5 |
| Minimum | 3 | 32 | 31 |
| Maximum | 5 | 36 | 36 |
| Sum | 88 | 1553 | 1547 |
| Count | 24 | 48 | 48 |

**DV** – Dorsal to ventral measurement

**LM** – Lateral to medial measurement

The empirical distribution of data measurements tends to represent a relatively "normal" population sample group. This group seems to be homogenous in terms of its representation of data criteria. These aspects are illustrated in the graphical illustrations below.
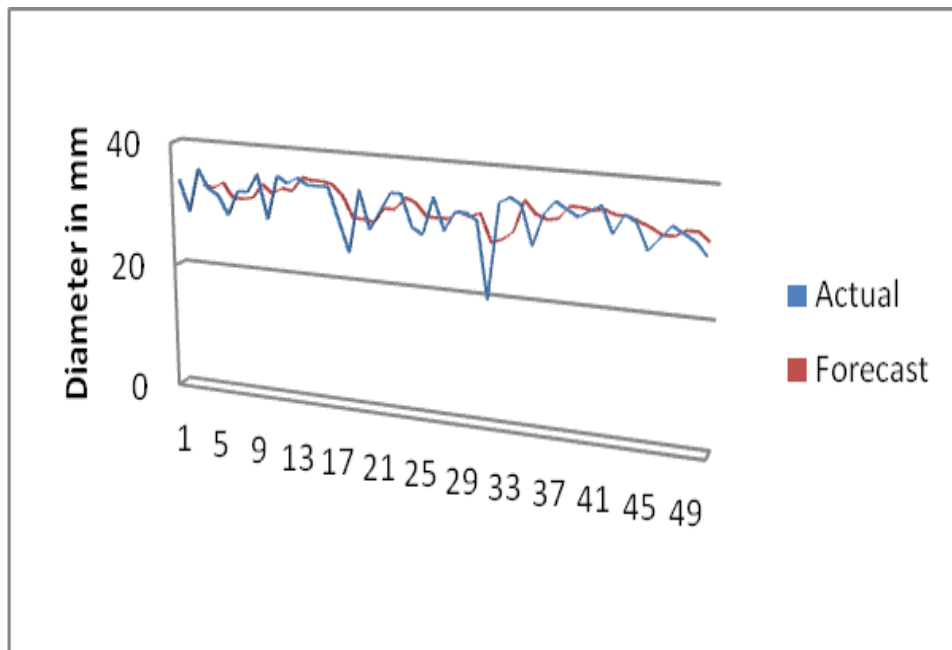


**Figure 5.3.** Globe measurements taken in millimetres from dorsal to ventral (vertical). The blue line represents the trend of actual sample measurements while the red line assumes a cumulative average over the population sample group

55
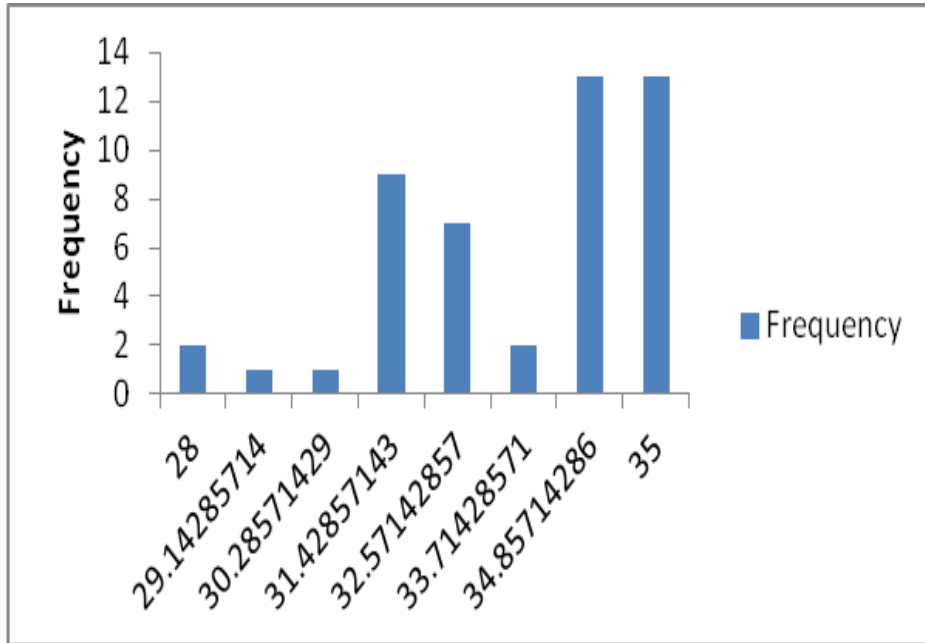
**Figure 5.4.** Histogram representing the freqency dispersion of vertical globe measurements over the sample population
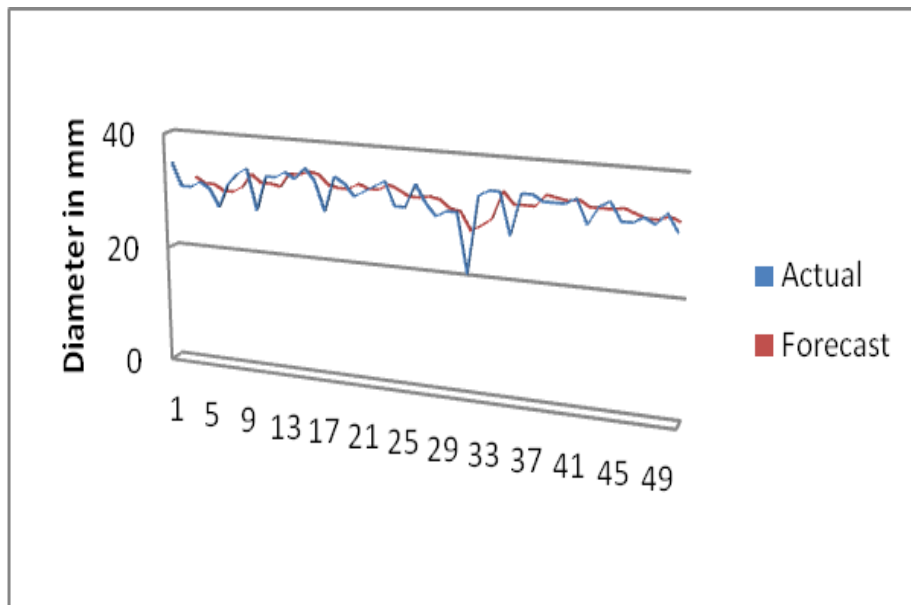


**Figure 5.5.** Globe measurements taken in millimetres from lateral to medial (horizontal). The blue line represents the trend of actual sample

56

measurements while the red line assumes an accumulative average over the population group
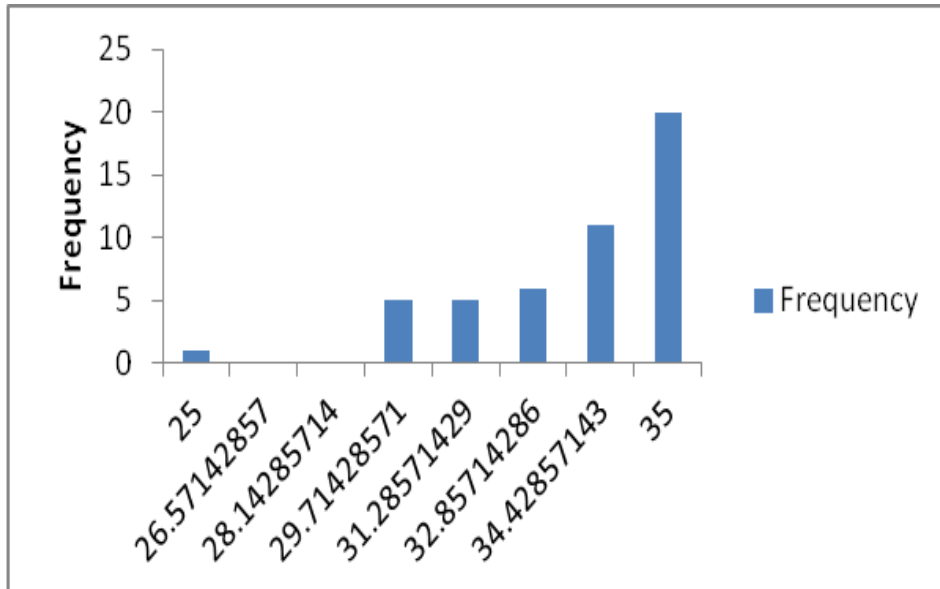


**Figure 5.6.** Histogram presenting the frequency distribution of horizontal globe measurements over the sampled population group

5.2 Rod to cone concentration

On analysis of data gained from the electron microscopy cell count, a marked difference was noted between the two topographically separate areas in the retinal tissue. Photoreceptor cell counts were taken from both lateral and medial to the optic nerve and statistically described.

Mean rod counts one optic disc space dorsomedial to the optic nerve averaged at 25.46 per field whereas in a similar location lateral to the optic nerve, mean values averaged at 20.08. Central tendency values for cone counts in these two locations differed more dramatically with mean values in

57

the medial location analysed at 3.04 and in the lateral location almost double the value at 6.38 Mean rod to cone ratios were also calculated and statistically relate to an uneven distribution between the two locations. A mean rod to cone ratio of 3.47 in the lateral sample as compared to 9.04 in the medial location.

Histograms generated from the data reflect relatively homogenous data with a close to normal dispersion of values. Slight assymmetry around the central tendency with skewness values of 0.1 – 0.8 are calculated.

The lateral rod to cone ratio values revealed a kurtosis of 0.26. This indicates a slight peak towards a central tendency or mean whereas the medial ratios tended to have a flatter distribution over the asymmetry around the mean. This value was calculated at -1.43.

This data is reflected in the tables and figures below.
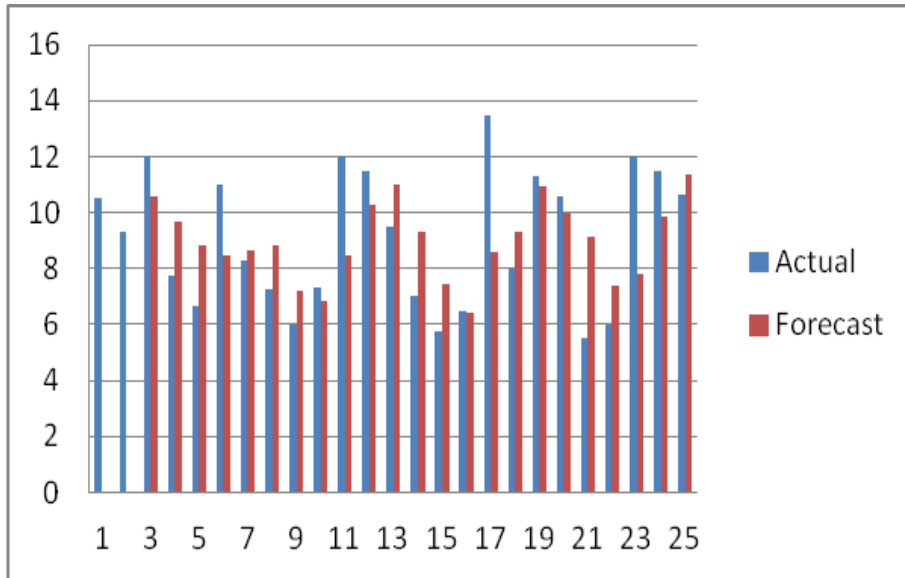
**Figure 5.7.** Bar histogram illustrating rod to cone ratio in the dorsomedial sample. The mean value for this calculation is 9.03

**Table 2.** Descriptive statistics calculated from rod and cone counts in the dorsomedial retinal location

| Variable | Rod Count | Cone Count | R/C |
|---|---|---|---|
| **Mean** | 25.45833 | 3.041667 | 9.039583 |
| **Standard Error** | 0.934405 | 0.175276 | 0.5038 |
| **Median** | 24 | 3 | 8.815 |
| **Mode** | 24 | 3 | 12 |
| **Standard Deviation** | 4.577631 | 0.858673 | 2.468105 |
| **Sample Variance** | 20.95471 | 0.737319 | 6.091543 |
| **Kurtosis** | -0.98414 | -0.52578 | -1.43904 |
| **Skewness** | 0.335248 | 0.365478 | 0.110503 |
| **Range** | 16 | 3 | 8 |
| **Minimum** | 18 | 2 | 5.5 |
| **Maximum** | 34 | 5 | 13.5 |
| **Sum** | 611 | 73 | 216.95 |
| **Count** | 24 | 24 | 24 |

**R/C** = Rod to cone ratio
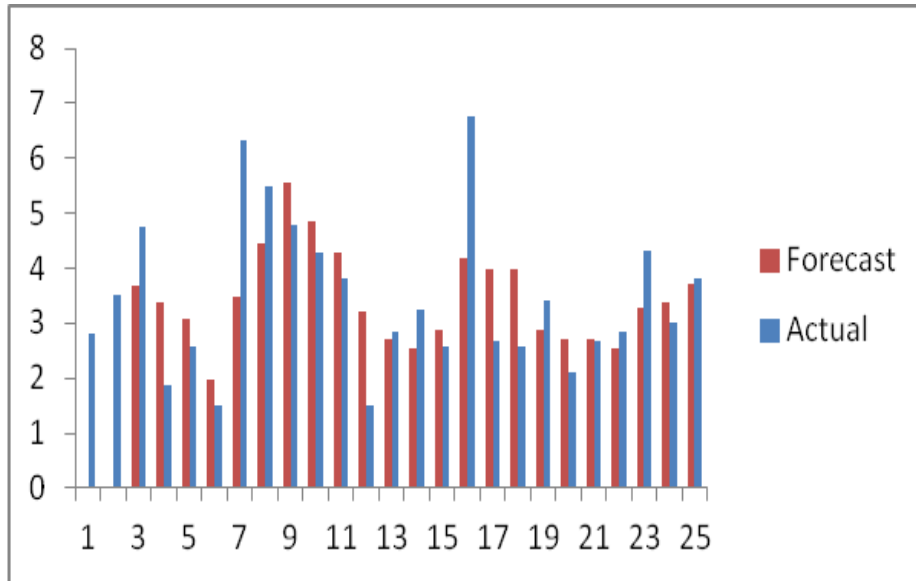
**Figure 5.8.** Histogram representing the rod to cone ratio in the dorsolateral sample location. The mean value for this topographical area was noted at 3.47

**Table 3.** Descriptive statistical data generated from the rod and cone counts in the dorsolateral retinal laocation

| Variable | Rod Count | Cone Count | R/C |
|---|---|---|---|
| Mean | 20.08333 | 6.375 | 3.4675 |
| Standard Error | 0.896686 | 0.370138 | 0.285894 |
| Median | 19 | 6 | 3.125 |
| Mode | 19 | 6 | 2.57 |
| Standard Deviation | 4.392847 | 1.813296 | 1.400588 |
| Sample Variance | 19.2971 | 3.288043 | 1.961646 |
| Kurtosis | -0.19709 | -0.63702 | 0.257314 |
| Skewness | 0.482889 | 0.100684 | 0.823059 |
| Range | 18 | 7 | 5.26 |
| Minimum | 12 | 3 | 1.5 |
| Maximum | 30 | 10 | 6.76 |
| Sum | 482 | 153 | 83.22 |
| Count | 24 | 24 | 24 |

**R/C** = Rod to cone ratio

5.3 Cone photopigment

The immunohistochemical cone photopigment study carried out was a qualitative and descriptive exercise classifying the presence or absence of specific photopigments.

One of three slides from each donor retina stained and examined for stain AB5407 (short wavelength/blue sensitive cones) were positive for this cone class.

Similarly the third of three slides from each donor stained and examined for stain AB5405 (medium wavelength/green sensitive cones) were also positive for this antigen-antibody interaction.

The second slide of three from each donor retinal sample stained and examined for stain AB5745 (long wavelength/red sensitive cones) appeared to be devoid of this complex.

# CHAPTER 6

## DISCUSSION

### 6.1 Discussion

#### 6.1.1 Globe Size

The eyes of all domestic animals studied and documented thus far seem to have fairly uniform shape, being spherical in most instances. The horizontal and vertical proportions tend to be nearly identical.[34] The average vertical measurement of the adult domestic cow eye is known to be 40.82mm and 41.90mm horizontally. The average measurements recorded in this study for the population of 3-5 year old African buffalo were significantly smaller (vertical 33.04mm and 32.91mm horizontal). The average ratio of 1:1,004 corresponds to the shape and proportions described for most adult domestic animals.[1]

#### 6.1.2 Rod and cone distribution in the retina

With all species studied to date, the distribution of photoreceptor cells across the retinal sheet is not homogenous. In this study there seems to be a distinct difference between two selected topographical areas in terms of rod and cone representations. This suggests that the African buffalo does, like all other species studied thus far, have a region synonymous to the *area centralis.*

In previous publications it is suggested there may to be a correlation between ganglion cell topography and spatial distribution of retinal photoreceptor cells.

62

A recent Japanese study involving a different species of buffalo (*Bos bubalis)* ganglion cell distribution was investigated. The highest concentration of ganglion cells was noted in the visual streak (dorsal to the optic disc). The distribution of ganglion cells varied in other areas of the retina, however was particularly concentrated in the dorsolateral region. This area corresponds to the cone rich *area centralis.* Average ganglion cell concentrations were noted in the dorsomedial retina and the lowest concentrations were observed in the ventral retina. Smaller ganglion cells were also observed in areas of higher concentration, specifically in the *area centralis*.

Ganglion cell densities have also recently been examined in the African elephant (*Loxodonta africana)*. Similar topographical distributions are described in this study, which also describes similar references to the black rhinoceros (*Dicerus bicornis).* [Pettigrew and Manger, 2008] and the equine [Evans and McGreevy, 2007]. We could potentially assume a similar rod and cone distribution in these species as well.

It would be reasonable to assume that the specialised dorsolateral retinal region in the African buffalo, that appears to be similar in nature to the *area centralis* and potentially also has a higher density of ganglion cells associated with it, subserves a similar function to that reported for other mammals with retinal specialisation. Hughes, in 1977 suggested that it allows animals to scan the horizon for either predators or conspecifics, the latter being a potentially important aspect in the social interactions of animals.

63

### 6.1.3 Cone photoreceptors

Classically, colour vision is considered to be a property of cones. More specifically, colour vision is determined by the number of photopigment classes to be found in the retina. The peak absorbances of cones in most domestic mammalian species studied to date seems to fall within the dichromatic colour spectral range.[37] The African buffalo seems no different.

In behavioral studies carried out in domestic cattle, known to be dichromates, visual clues have been shown to be more important than auditory clues particularly in acquiring food.[11] The buffalo being active grazers in mostly high ambient lighting conditions and at dusk and dawn, would require a degree of colour vision suited to its environment and behavior.[33]

### 6.2 Conclusion

This study has shown that the African buffalo like other mammals studied to date does not have a uniform retina in terms of rod and cone distribution. Rod to cone ratios do vary topographically.

The African buffalo retina does also have a specialised region contained in its retina that appears to be similar in nature to the *area centralis* found and described in other species. In this region a lower rod to cone ratio is observed and is typically located dorsolateral to the optic nerve.

The African buffalo has a short wavelength cone population, with maximal absorption of 435-455nm and a middle/long wavelength cone population with

a peak absorbance of 530-555nm. This study shows that their colour vision is comparable to that of other domestic animals and deuteranopes, or humans missing the green cone population.

# REFERENCES

1.  SAMUELSON, D.A. Ophthalmic Anatomy. In: GELATT, K.N., ed. *Veterinary Ophthalmology.* Third ed. Philadelphia: Lippincott (1999; 31-150).

2.  SIMS, M.H. Electrodiagnostic Evaluation of Vision. In: GELATT, K.N., ed. *Veterinary Ophthalmology.* Third ed. Philadelphia: Lippincott (1999; 483-507).

3.  NARFSTROM, K. (1985). Progressive retinal atrophy in the Abyssinian cat: Clinical Characteristics. *Investigative Ophthalmology Visual Science.* 26, 193.

4.  WALDVOGEL, J.A. (1990). The bird's eye view. *American Scientist.* 78, 342-353.

5.  OFRI, R. Optics and Physiology of vision. In: GELATT, K.N., ed. *Veterinary Ophthalmology.* Third ed. Philadelphia: Lippincott (1999; 183-216).

6.  GUENTHER, E. & ZRENNER, E. (1993). The spectral sensitivity of dark and light adapted cat retinal ganglion cells. *Journal of Neuroscience.* 13, 1543-1550.

7.  SZEL, A. ROHLICH, P., CAFFE, A.R., JULIUSSON, B., AGUIRRE, G. & VAN VEEN, T. (1992). Unique topographic separation of two spectral classes of cones in the mouse retina. *Journal of comparative Neurology.* 352, 327

8.  WILKER, V.H., WILLIAMS, R.W. & RAKIC, P. (1990). Photoreceptor Mosaic: Number and distribution of rods and cones in the rhesus monkey retina. *Journal of Comparative Neurology.* 297, 499.

9.  MILLER, P.E. (1996). A limited review of feline and equine vision. *Trans American College Veterinary Ophthalmology.* 26, 94-102.

10. DOWLING, J. (1987). Visual adaptation and photoreceptor mechanisms. In: DOWLING, J., ed. *The Retina.* Cambridge: Belknap Press of Harvard University. 187-223.

11. BRINDLEY, G.S. (1970). The photochemistry of the retina. In: BRINDLEY, G.S., ed. *Physiology of the retina and visual pathway.* 2nd ed. London: Edward Arnold Publishers. 1-46.

12. SAARI, J.C. (1992). The biochemistry of sensory transduction in vertebrate photoreceptors. In: HART, W.M. JR., ed. *Adler's Physiology of the eye.* 9th ed. St. Louis: Mosby-Year Book. 460-484

13. SAARI, J.C. (2000). Biochemistry of visual pigment regeneration: The Friedenwald Lecture. *Investigative Ophthalmology Visual Science.* 41, 337-348.

14. EDWARDS, R.B. & ADLER, A.J. (2000). IRBP enhances removal of 11-*cis*-retinaldehyde from isolated RPE membranes. *Experimental Eye Research.* 70, 235-451.

15. HORWITZ, J. & HELLER, J. (1973). Interactions of all-*trans*-, 9-, 11-, and 13-*cis*-retinal, all-*trans*-retinyl acetate, and retinoic acid with human retinal-binding protein and prealbumin. *Journal of Biological Chemistry.* 248, 6317-6324.

16. TSCHANZ, C.L. & NOY, N. (1997). Binding of retinol in both retinoid-binding sites of interphotoreceptor retinoid-binding protein (IRBP) is stabilised mainly by hydrophobic interactions. *Journal of Biological Chemistry.* 272, 30201-30207.

17. JACOBS, G.H. (1993). The distribution and nature of colour vision among mammals. *Biological Reviews* 68, 413-471.

18. JACOBS, G.H. (1981). *Comparative colour vision.* Academic Press, New York.

19. FOSTER, S.J. (2000). Vision in the dog (*Canis familiaris)* with references to the domestic cat (*Felis catus). Veterinary International.* 12, 2, 2-10.

20. RIOL, J.A., SANCHEZ, J.M., EGUREN, V.G. & GUADIOSO, V.R. (1989). Colour perception in Fighting Cattle. *Applied Animal Behaviour Science.* 23, 199-206.

21. GILBERT JR., B.J. & ARAVE, C.W. (1986). Ability of cattle to distinguish among different wavelengths of light. *Journal of dairy science.* 69, 825-832.

22. JACOBS, G.H., DEEGAN II, J.F. & NEITZ, J. (1998). Photopigment basis for dichromatic colour vision in cows, goats and sheep. *Visual Neuroscience* 15, 581-584.

23. ROBERTS, S.M. (1992). Equine vision and optics. *Veterinary Clinics of North America: Equine Practice* 8, 3, 451-457.

24. TIMNEY, B. & KEIL, K. (1992). Visual acuity in the horse. *Vision research.* 32, 12, 2289-2293.

25. KOLB, H. (1994). The architecture of the functional neural circuits in the vertebrate retina. *Investigative Ophthalmology Visual Science.* 35, 2385.

26. BOYCOTT, B. & RAVIOLA, E. (1999). Parallel processing in the mammalian retina. *Investigative Ophthalmology Visual Science.* 40, 1313.

27. ANDERSON, D.H., FISHER, W.H. & STEINBERG, R.H. (1978). Mammalian cones: Disc shedding, phagocytosis and renewal. *Investigative Ophthalmology Visual Science.* 17, 117.

28. UETAKE, K., & KUDO, Y. (1994). Visual dominance over hearing in feed acquisition procedure in cattle. *Applied Animal behavioural Science.* 42, 1-9.

29. DABROWSKA, B., HARMATA, W., LENKIEWICZ, Z., SCHIFFER, Z. & WOJTUSIAK, R.J. (1981). Colour perception in cows. *Behavioural Processes.* 6, 1-10.

30. ADLER, A.J. & EVANS, C.D. (1985). Some functional characteristics of purified bovine interphotoreceptor retinal-binding protein. *Investigative Ophthalmology Visual Science.* 26, 273-282.

31. ADLER, A.J, EVANS, C.D. & STAFFORD III, W.F. (1985). Molecular -
properties of bovine interphotoreceptor retinal-binding protein. *Journal of Biological Chemistry.* 260, 4850-4855.

32. FONG, S.L., LIOU, G.I., LANDERS, R.A., ALVAREZ, R.A. & BRIDGES, C.D. (1984). Purification and characterisation of a retinal-binding glycoprotein synthesised and secreted by bovine neural retina. *Journal of Biological Chemistry.* 259, 6534-6542.

33. NARFSTROM, K., EHINGER, B. & BRUUN, A. (2001). Immunohistochemical studies of cone photoreceptors and cells of the inner retina in feline rod-cone degeneration. *Veterinary Ophthalmology* 4, 2, 141-145.

34. BELTRAN, W. (2006). A frameshift mutation in RPGR exon ORF15 causes photoreceptor degeneration and inner retina remodeling in a model of X-linked retinitis pigmentosa. *Ophthalmology Visual. Science.* 47, 1669-1681.

35. SRINIVAS, M. (2006). Activation of the blue opsin gene in cone photoreceptor development by retinoid-related orphan receptor beta. *Molecular Endocrinology* 20, 1728-1741.

71

36. ROBERTS, R., MELANIE, R. (2005). Retinoid X receptor (gamma) is necessary to establish the S-opsin gradient in cone photoreceptors of the developing mouse retina. *Investigative Ophthalmology Visual Science* 46, 2897-2904.

37. JACQUEMIN,E., JONET, L., OLIVER, L., BUGRA, K., LAURENT, M., COURTOIS, Y., JEANNY, J. (1993) Developmental regulation of acidic fibroblast growth factor (aFGF) expression in the bovine retina. *Journal of Developmental Biology* 37,3,417-423.

# APPENDIX 1

## PROVISIONAL PROTOCOL

## MAY 2005

## 1.    INTRODUCTION

According to the program schedule for the course MMedVet (Ophth), set out for Dr LT Odayar, the research methodology course is to take place in June/July 2005. By the end of the course, in December 2005, the protocol for the research project to be undertaken should in effect be complete.

The proposed topic for the research project will deal with investigating certain aspects of vision in the African buffalo. This will include quantifying the photoreceptor composition and Immunohistochemical evaluations of the retina.

Fresh buffalo eye specimens will be required to carry out these studies as accurately as possible. In speaking with various authorities including wildlife veterinarians, we understand that many buffalo will be culled especially during the upcoming winter period, commencing in May 2005. We have also been informed that the eyes of these animals are not being used by any other research venture and are thus available for such use. Authorities involved in

73

this process have agreed to donate these eyes for this proposed research project and hence to the benefit of scientific progress and knowledge.

Since buffalo eye specimens will become available before the completion and approval of the final protocol, this provisional protocol / letter, has the purpose to seek permission to collect these specimens in the meantime, to avoid the unfortunate wastage of valuable resources.

## 2. METHOD

## 2.1 HARVESTING THE SPECIMENS

As soon as possible after the buffalo has been shot the eyes will be enucleated using the standard subconjunctival approach without performing a lateral canthotomy so as to preserve the surrounding skin and eyelids. A brief description of the proposed procedure follows.

To facilitate exposure of the globe, eyelid retractors will be used to separate the eyelid margins. Beginning in a dorsal quadrant, the bulbar conjunctiva will be incised approximately 5mm posterior to the limbus. The conjunctiva and Tenon's capsule will be bluntly dissected from the globe. The extraocular muscles will be identified and transected close to their scleral insertions. The globe will then be mobilised and displaced in a forward direction. The retractor bulbi muscle will then be transected in a similar fashion. The globe will then be rotated medially to expose the optic nerve, which will be clamped with a

74

curved haemostat. The nerve will be transected 5mm behind the posterior end of the globe. The haemostat will then be removed. The orbit will be packed with cotton wool swabs to control any minor haemorrhages. These will then be removed.

## 2.2   PROCESSING THE SPECIMENS

Once removed, one eye will immediately be placed into a glutaraldehyde bath. A horizontal incision, through the optic nerve, will then be made through the eyeball while immersed in glutaraldehyde. The vitreous will be allowed to flow out. Each half of the globe will be pinned to a polystyrene base immersed in glutaraldehyde and with blunt forceps the retina will be gently peeled away from the inner posterior surfaces of each half of the globe. The retinas will be placed in glutaraldehyde containing specimen bottles and submitted to the Electron Microscopy Unit for further processing and cutting, in preparation for the scanning electron microscope examination.

The other eye, from the same animal, will be trimmed of excess extraocular tissue (muscle and fat). The eyeball will then be immersed in 10% buffered formalin and fixed over a period of 48-72hrs. This specimen will then be submitted to the pathology laboratory for further processing and cutting in the preparation for light microscopy examination.

75

## 3. PROPOSED BUDGET

- Travelling costs @ standard SAVA rates      R    2 201.67

  (1 trip of 1439km   @ R1.53/km)

- Toll fees      R    216.00

- Accommodation @ R100per person      R    200.00

- Digital camera @ no cost      R    0.00

- Surgical instruments @no cost      R    0.00

- Pins      R    5.00

- 1 box of examination gloves      R    25.00

- Cooler box @ no cost      R    0.00

- 30 litres of glutaraldehyde @ R0.00/litre      R    0.00

- Scanning electron microscopy      R    1 500.00

  (50 specimens x 5 photo negatives @ R 6.00 each)

- Scanning electron photographic prints      R    260.00

  (20 @ R13.00 each)

- 10 litres of formalin @ R3.10/litre      R    31.00

- 30 Specimen bottles @ R0.42 each      R    12.60

- Light microscopy      R    300.00

  (15 specimens @ R20/section)

- 2 Reams of paper @ R35.00 each      R    70.00

- 10 re-writable CD's @ R5.00 each      R    50.00

- 20 Digital photo prints @ R2.50 each      R    50.00

- Immunohistochemical stains      R    2 000.00

- Publication costs – Reproduction of colour

photographic prints       R 1 000.00

            **Total R 8 000.00**

# APPENDIX 2

## SPECIMEN DATA

| DATE | DONOR IDENTITY | DONOR GENDER | DONOR AGE | LEFT GD-DV | LEFT GD-LM | RIGHT GD-DV | RIGHT GD-LM |
|---|---|---|---|---|---|---|---|
| 10/08/05 | 181 | FEMALE | 4y | 35 | 35 | 34 | 35 |
| 10/08/05 | 186 | FEMALE | 3y | 30 | 32 | 29 | 31 |
| 10/08/05 | 194 | MALE | 5y | 33 | 30 | 36 | 31 |
| 10/08/05 | 179 | MALE | 3y | 33 | 31 | 33 | 32 |
| 10/08/05 | 189 | MALE | 4y | 32 | 31 | 32 | 31 |
| 10/08/05 | 184 | MALE | 4y | 20 | 21 | 29 | 28 |
| 10/08/05 | 196 | MALE | 3y | 35 | 34 | 33 | 32 |
| 10/08/05 | 192 | MALE | 3y | 36 | 35 | 33 | 34 |
| 10/08/05 | 193 | MALE | 3y | 35 | 35 | 36 | 35 |
| 10/08/05 | 185 | FEMALE | 3y | 29 | 28 | 29 | 28 |
| 10/08/05 | 190 | FEMALE | 4y | 34 | 35 | 36 | 34 |
| 10/08/05 | 188 | FEMALE | 5y | 36 | 35 | 35 | 34 |
| 10/08/05 | 187 | FEMALE | 5y | 35 | 34 | 36 | 35 |
| 10/08/05 | 186 | FEMALE | 5y | 34 | 34 | 35 | 34 |
| 10/08/05 | 183 | MALE | 3y | 35 | 34 | 35 | 36 |
| 10/08/05 | 182 | MALE | 3y | 36 | 35 | 35 | 34 |
| 11/08/05 | 199 | FEMALE | 4y | 32 | 31 | 30 | 29 |
| 11/08/05 | 201 | MALE | 5y | 35 | 34 | 25 | 35 |
| 11/08/05 | 200 | MALE | 3y | 34 | 35 | 35 | 34 |
| 11/08/05 | 207 | MALE | 5y | 30 | 32 | 29 | 32 |
| 11/08/05 | 206 | FEMALE | 4y | 32 | 32 | 32 | 33 |
| 11/08/05 | 204 | FEMALE | 3y | 34 | 33 | 35 | 34 |
| 11/08/05 | 208 | FEMALE | 3y | 33 | 32 | 35 | 35 |
| 11/08/05 | 202 | FEMALE | 5y | 32 | 34 | 30 | 31 |
| 11/08/05 | 203 | MALE | 4y | 30 | 31 | 29 | 31 |

| KEY | |
|---|---|
| GD-DV | GLOBE DIAMETER DORSAL TO VENTRAL (mm) |
| GD-LM | GLOBE DIAMETER LATERAL TO MEDIAL (mm) |

## ELECTRON MICROSCOPY DATA TABLE

| DONOR IDENTITY | LS RODS | LS CONES | LS R/C | MS RODS | MS CONES | MS R/C |
|---|---|---|---|---|---|---|
| 181 | 14 | 5 | 2.8 | 21 | 2 | 10.5 |
| 186 | 21 | 6 | 3.5 | 28 | 3 | 9.33 |
| 194 | 19 | 4 | 4.75 | 24 | 2 | 12 |
| 179 | 15 | 8 | 1.87 | 31 | 4 | 7.75 |
| 189 | 18 | 7 | 2.57 | 20 | 3 | 6.67 |
| 184 | - | - | - | - | - | - |
| 196 | 19 | 3 | 6.33 | 25 | 3 | 8.3 |
| 192 | 22 | 4 | 5.5 | 29 | 4 | 7.2 |
| 193 | 24 | 5 | 4.8 | 30 | 5 | 6 |
| 185 | 30 | 7 | 4.29 | 22 | 3 | 7.33 |
| 190 | 19 | 5 | 3.8 | 24 | 2 | 12 |
| 188 | 12 | 8 | 1.5 | 23 | 2 | 11.5 |
| 187 | 17 | 6 | 2.83 | 19 | 2 | 9.5 |
| 186 | 26 | 8 | 3.25 | 21 | 3 | 7 |
| 183 | 23 | 9 | 2.56 | 23 | 4 | 5.75 |
| 182 | 27 | 4 | 6.76 | 26 | 4 | 6.5 |
| 199 | 16 | 6 | 2.67 | 27 | 2 | 13.5 |
| 201 | 18 | 7 | 2.57 | 32 | 4 | 8 |
| 200 | 117 | 5 | 3.4 | 34 | 3 | 11.3 |
| 207 | 19 | 9 | 2.11 | 32 | 3 | 10.6 |
| 206 | 16 | 6 | 2.67 | 22 | 4 | 5.5 |
| 204 | 20 | 7 | 2.86 | 18 | 3 | 6 |
| 208 | 26 | 6 | 4.33 | 24 | 3 | 12 |
| 202 | 24 | 8 | 3 | 23 | 2 | 11.5 |
| 203 | 19 | 5 | 3.8 | 32 | 3 | 10.67 |

| KEY | |
|---|---|
| LS | RETINAL SAMPLE ONE OPTIC DISC DIAMETER DORSOLATERAL TO OPTIC NERVE |
| MS | RETINAL SAMPLE ONE OPTIC DISC DIAMETER DORSOMEDIAL TO OPTIC NERVE |
| R/C | ROD: CONE |

# APPENDIX 4

## IMMUNOHISTOCHEMISTRY DATA TABLE

| DONOR IDENTITY | SLIDE NO. | STAIN 1 Y/N | STAIN 2 Y/N | STAIN 3 Y/N |
|---|---|---|---|---|
| 181 | 1 -3 | Y | N | Y |
| 186 | 4-6 | Y | N | Y |
| 194 | 7-9 | Y | N | Y |
| 179 | 10-12 | Y | N | Y |
| 189 | 13-15 | Y | N | Y |
| 184 | - | - | - | - |
| 196 | 16-18 | Y | N | Y |
| 192 | 19-21 | Y | N | Y |
| 193 | 22-24 | Y | N | Y |
| 185 | 25-27 | Y | N | Y |
| 190 | 28-30 | Y | N | Y |
| 188 | 31-33 | Y | N | Y |
| 187 | 34-36 | Y | N | Y |
| 186 | 37-39 | Y | N | Y |
| 183 | 40-42 | Y | N | Y |
| 182 | 43-45 | Y | N | Y |
| 199 | 46-48 | Y | N | Y |
| 201 | 49-51 | Y | N | Y |
| 200 | 52-54 | Y | N | Y |
| 207 | 55-57 | Y | N | Y |
| 206 | 58-60 | Y | N | Y |
| 204 | 61-63 | Y | N | Y |
| 208 | 64-66 | Y | N | Y |
| 202 | 67-69 | Y | N | Y |
| 203 | 70-72 | Y | N | Y |

| KEY | |
|---|---|
| STAIN 1 | AB5407 – BLUE OPSIN |
| STAIN 2 | AB5745 – RED OPSIN |
| STAIN 3 | AB5405 – GREEN OPSIN |

80